Cellular/Molecular

Heterogeneity of Ca^{2+}-Permeable AMPA/Kainate Channel Expression in Hippocampal Pyramidal Neurons: Fluorescence Imaging and Immunocytochemical Assessment

Fumio Ogoshi[1] **and John H. Weiss**[1,2,3]

Departments of [1]Anatomy and Neurobiology, [2]Neurology, and [3]Neurobiology and Behavior, University of California Irvine, Irvine, California 92697-4292

The presence of Ca^{2+}-permeable AMPA/kainate (Ca-A/K) channels on hippocampal pyramidal neurons (HPNs) has been controversial, although they are present on many forebrain GABAergic neurons. We combined high-resolution fluorescence Ca^{2+} imaging with surface AMPA receptor (AMPAR) subunit immunocytochemistry to examine the expression of functional Ca-A/K channels in dissociated hippocampal neurons at the subcellular level. In GABAergic neurons [identified by glutamate decarboxylase (GAD) immunocytochemistry], focal application of AMPA induced large dendrosomatic intracellular $[Ca^{2+}]$ ($[Ca^{2+}]_i$) rises, consistent with their known strong Ca-A/K channel expression. Surface immunostaining for the AMPAR subunits GluR1 and GluR2 revealed abundant dendritic GluR1 puncta containing little or no GluR2, which, when present, was limited to diffuse staining in the soma and proximal dendrites. In contrast, the majority of HPNs (putatively identified by morphological criteria and lack of GAD labeling) showed little or no AMPA-induced $[Ca^{2+}]_i$ rise. Correspondingly, most HPNs showed strong dendritic labeling for both GluR1 and GluR2 that colocalized extensively. A subpopulation of HPNs, however, displayed noticeable $[Ca^{2+}]_i$ rises that began and often reached their highest levels in discrete dendritic regions. In these HPNs, levels of GluR1 relative to GluR2 were higher, and GluR1 was often present without overlying GluR2. The present studies, which are the first to directly examine the relationship between the local complement of cell surface AMPAR and the presence of dendritic Ca-A/K channels, clearly indicate that considerable cell surface GluR2 does not preclude the presence of Ca-A/K channels and further show that HPNs display considerable heterogeneity in terms of apparent Ca-A/K channel expression.

Key words: calcium; hippocampus; dendrite; AMPA; GluR1; GluR2

Introduction

AMPA/kainate-type glutamate receptors mediate most fast excitatory transmission in the CNS. Whereas most of these channels are Ca^{2+}-impermeable, certain neurons possess AMPA/kainate channels that are directly permeable to Ca^{2+} (Ca-A/K channels). Ca-A/K channels appear to be comprised of combinations of three AMPA subunits [Glu receptors (GluRs) 1, 3, and 4] but lack the GluR2 subunit, which prevents Ca^{2+} permeability in heteromeric channels (Hollmann et al., 1991; Verdoorn et al., 1991). Although forebrain GABAergic neurons often possess large numbers of Ca-A/K channels (McBain and Dingledine, 1993; Bochet et al., 1994; Jonas et al., 1994; Yin et al., 1994), their presence on hippocampal pyramidal neurons (HPNs), has been controversial, with both electrophysiological studies and evidence of strong

GluR2 expression arguing against a substantial presence of these channels (Jonas et al., 1994; Geiger et al., 1995; Spruston et al., 1995; Garaschuk et al., 1996; Petralia et al., 1997). However, recent studies raised the possibility that limited numbers of Ca-A/K channels may be present on HPNs, perhaps particularly at synaptic sites away from the soma, where they would be difficult to detect with whole-cell recordings, but may have important physiological functions (Pruss et al., 1991; Lerma et al., 1994; Wenthold et al., 1996; Toomim and Millington, 1998; Yin et al., 1999).

Although the physiological significance of Ca-A/K channels has been uncertain, dendritic AMPA receptors (AMPARs) can turn over rapidly in response to physiological stimulation, raising the possibility that numbers of Ca-A/K channels are dynamically regulated. In addition, these channels are selectively permeable to Zn^{2+}, suggesting that they may have a particular role in mediating signaling by this synaptically released cation (Weiss and Sensi, 2000; Jia et al., 2002). Moreover, accumulating evidence suggests that Ca-A/K channels play a role in disease-associated neurodegeneration. Indeed, in the case of HPNs, irrespective of their presence under basal conditions, evidence that levels of GluR2 decrease after transient ischemia or epilepsy lent support to the "GluR2 hypothesis," which suggests that a consequent increase in

Ca-A/K channel numbers contributes to the delayed neurodegeneration often seen in these conditions (Pellegrini-Giampietro et al., 1992; Tanaka et al., 2000).

Several approaches have been used to examine the presence of neuronal Ca-A/K channels. Many past studies have made inferences based on methods such as AMPAR *in situ* hybridization and immunocytochemistry, which do not provide direct information as to the presence of functional channels. Alternatively, methods that permit the detection of functional Ca-A/K channels include labeling by a histochemical technique (based on kainate-stimulated uptake of Co^{2+} ions; Pruss et al., 1991), fluorescent imaging (Yin et al., 1999; Vandenberghe et al., 2001), and electrophysiological recordings to assess rectification of whole-cell currents (Iino et al., 1990, 1994; Lerma et al., 1994; Isa et al., 1996).

To date, however, no study has correlated the distribution of cell surface AMPAR subunits with the local presence of Ca-A/K channels in the soma and dendrites of individual neurons. To this aim, the present study combines high-resolution fluorescent Ca^{2+} imaging to detect Ca-A/K channels on cultured hippocampal neurons with immunocytochemical detection of cell surface GluR1 and GluR2 subunits and seeks to make a comparison between HPNs and GABAergic neurons. The present findings indicate that in each of these cell types, both subunits are often present in the somata, and the presence of considerable dendritic GluR1 relative to GluR2 predicts the presence of Ca-A/K channels. In addition, although Ca-A/K channels were only detected in a subset of HPNs, when present, their expression patterns and intracellular Ca^{2+} responses to activation differed from those in GABAergic neurons in ways that may point toward differences in the nature of Ca-A/K channel-mediated divalent cation signaling between these cell types.

Materials and Methods

Chemicals and reagents. Fluo-4ff AM was purchased from Molecular Probes (Eugene, OR). 1-Naphthyl acetyl spermine (NAS) was kindly provided by Daicel Chemical (Tokyo, Japan). AMPA was purchased from Tocris (Ellisville, MO). Dizocilpine maleate (MK-801) was purchased from Research Biochemicals (Natick, MA). Kainate was purchased from Ocean Produce International (Shelburne, Nova Scotia). Tissue culture media and supplements were supplied by Invitrogen (Carlsbad, CA). Most other chemicals and reagents were obtained from Sigma (St. Louis, MO).

Pure hippocampal neuronal cultures. All animal procedures were conducted in accordance with the National Institutes of Health *Guide for the Care and Use of Laboratory Animals* and approved by the University of California Irvine Institutional Animal Care and Use Committee. Hippocampal neuronal cultures containing very little glia ($\sim$5–10%) were prepared from embryonic day 18 Sprague Dawley rats (Simonsen, Santa Clara Valley, CA) as previously described (Brewer et al., 1993). Briefly, the hippocampi were removed and dissociated by trituration after trypsin treatment. Neurons were plated in Neurobasal medium with 2% B27 (medium supplement containing fatty acids, antioxidants, vitamins, and hormones) (NB-B27), supplemented with 0.5 mM glutamine and 25 μM glutamate, at 1×10^5 cells per 35 mm dish, on poly-D-lysine-coated, glass-bottom imaging dishes (MatTek Corp., Ashland, MA). Cultures were maintained in NB-B27 supplemented with 0.5 mM glutamine and were typically used between 14 and 21 d *in vitro*.

Co^{2+} labeling. Co^{2+} uptake labeling of cultured neurons was performed as described previously for murine cultures (Yin et al., 1994), with minor modifications. After Co^{2+} loading (by exposure to 100 μM kainate with 5 mM Co^{2+} in PBS for 5 min), intracellular Co^{2+} was precipitated with 0.05% (NH$_4$)$_2$S for 2 min. The cultures were then washed and fixed in cold methanol for 5 min, and the staining was enhanced by a modified Timm's stain procedure. Demonstrating the specificity of this method in rat cultures, Co^{2+} staining was not observed if

NMDA (100 μM) or high (60 mM) K$^+$ [to directly activate the voltage sensitive Ca^{2+} channel (VSCC)] was substituted for kainate, and the labeling was completely blocked by the AMPA/kainate antagonist 2,3-dihydroxy-6-nitro-7-sulfonyl-benzo[f]quinoxaline (data not shown).

Ca^{2+} imaging. Cultures were loaded in the dark with 5 μM of the AM ester of the low-affinity Ca^{2+} probe fluo-4ff (K_d, 9.7 μM) in HEPES-buffered salt solution (HSS; in mM: 130 Na$^+$, 5.4 K$^+$, 0.8 Mg^{2+}, 1.8 Ca^{2+}, 130.6 Cl$^-$, 20 HEPES, and 15 glucose, pH 7.4) containing 0.2% pluronic acid and 1.5% dimethylsulfoxide for 30 min at 25°C, washed in HSS, and then kept in the dark for 30 min for dye de-esterification. Cultures were then mounted to a stage adapter on an inverted microscope (Diaphot; Nikon, Mellville, NY) equipped with a 75W xenon lamp, a computer-controlled filter wheel, a 40× epifluorescence oil immersion objective, and a green fluorescence cube (excitation, 490 nm; dichroic, 510 nm; emission, 530 nm). Fields were selected containing an average of one or two neurons that were sufficiently isolated from other neurons that their dendritic arborizations could be distinctly resolved, and images were acquired using a 12-bit cooled digital CCD camera (Hamamatsu, Bridgewater, NJ) and MetaFluor 4.0 software (Universal Imaging, West Chester, PA). The fluorescence increase over baseline (ΔF) was calculated as F_x/F_0, where F_x indicates the fluorescence at time x, and F_0 indicates the average baseline fluorescence for the same region. Pseudo-color images of ΔF values were generated using MetaMorph software. AMPA applications [25 μM, 1 sec, room temperature, with 10 μM of both the NMDA blocker MK-801 and the VSCC blocker Gd^{3+}, with or without NAS (300 μM) or 1-(aminophenyl)-methyl-7,8-methylendioxil-5H-2,3-benzodiazepine (GYKI 52466) (100 μM)] were via glass micropipettes (tip opening, $\sim$15 μm) attached to a pneumatic pressure system (PPS-2; Medical Systems, Great Neck, NY). The tip of the puffer pipette was placed 250 μm above and 250 μm outside the 400× microscope field and angled at 45° above the horizontal. Calibration experiments indicated that, under these conditions, a 1 sec pulse of color dye always fully covers the field. The applied drug solution was rapidly cleared by a suction pipette placed directly across the field.

Immunocytochemistry. For glutamate decarboxylase (GAD), Ca^{2+}/calmodulin-dependent protein kinase IIα (CaMKIIα), or synaptophysin labeling, cells were fixed in cold methanol at -4°C for 10 min, washed, blocked for 1 hr (5% goat serum in PBS), and incubated in rabbit anti-GAD-67 antibody (1:1000; Chemicon, Temecula, CA), mouse anti-CaMKIIα antibody (1:1000; Chemicon), or rabbit anti-synaptophysin antibody (1:200; Stressgen Biotechnologies Corp.) in 0.2% Triton X-100 for 1 hr. Cultures were then incubated for 1 hr with either a biotinylated secondary antibody (for GAD labeling, 1:100; Vector Laboratories, Burlingame, CA), or with a fluorescent secondary antibody (for synaptophysin labeling, 1:200 goat anti-rabbit Alexa Fluor 594; for GAD and CaMKIIα double labeling, 1:200 goat anti-rabbit Alexa Fluor 594 and goat anti-mouse Alexa Fluor 488; Molecular Probes). After washing in PBS, GAD labeling was visualized using ABC solution (Vector Laboratories) and 3-amino-9-ethyl-carbazole, and combined GAD and CaMKIIα or synaptophysin labeling was visualized under fluorescence microscopy.

For AMPAR subunit and GAD triple-fluorescence labeling, live hippocampal neurons were washed in HSS and incubated at 37°C for 20 min with mouse anti-GluR2 N-terminal antibody (1:25; Becton Dickinson, Pharmingen, San Diego, CA) and rabbit anti-GluR1 N-terminal antibody (1:50; a generous gift from R. L. Huganir, Howard Hughes Medical Institute and Department of Neuroscience, Johns Hopkins School of Medicine, Baltimore, MD). After quick washes, the neurons were fixed in cold methanol for 10 min, washed, incubated in secondary antibodies conjugated to fluorophores (1:100, goat anti-mouse Alexa Fluor 594; and 1:100, Fab fragment goat anti-rabbit FITC; Jackson ImmunoResearch, West Grove, PA) for 1 hr at room temperature, and then washed thoroughly. The cultures were further processed for GAD staining as above, except visualization was achieved by incubating 1 hr with goat anti-rabbit aminomethylcoumarin-conjugated secondary antibody (1:100; Jackson ImmunoResearch). The use of a Fab fragment secondary antibody for GluR1 allowed for the use of a second rabbit primary antibody for GAD. Fluorescent images were acquired using the same apparatus described above for Ca^{2+} imaging, with acquisition settings for each antibody that were maintained across experiments, and images (single fluorophore and

pseudocolor overlays) were generated using Photoshop (Adobe Systems Inc., San Jose, CA). Because subtle procedural variability could cause some experiment-to-experiment variation in the relative intensities of GluR1 and GluR2 staining, in each experiment, the range of labeling intensities for each subunit across the population of neurons was carefully evaluated to ascertain that the full range of staining patterns, comparable with that seen in other dishes, was present before making assessments of staining patterns in individual neurons.

Quantitative assessment of GluR1 and GluR2 surface staining. After Ca²⁺ imaging and triple immunolabeling (for GAD, GluR1, and GluR2), putative GAD(−) HPNs were classified as either Ca-A/K(+) or Ca-A/K(−) on the basis of imaging responses [Ca-A/K(+); somatic ΔF, >2.0 within 15 sec) and then analyzed in two ways to assess relative GluR1 and GluR2 surface staining. In the first, average fluorescence intensity for each subunit in the dendrites was assessed by tracing a region around the dendrites clearly linked to a single neuron (but omitting the soma and very proximal dendrites) using MetaMorph software and measuring the average fluorescence intensity (eight bit raw intensity values) for each subunit in the selected regions. The other approach was based on direct counting of discrete dendritic puncta, which were categorized as either showing stronger GluR1 than GluR2 fluorescence (GluR1 > GluR2; note that this includes puncta showing GluR1 only) or showing GluR2 fluorescence that was stronger or equal to that of GluR1 (GluR2 ≥ GluR1).

Quantitative measures and statistics. All quantitative measures comprise data from a minimum of four separate culture preparations and are expressed as means ± SEM. Statistical significance of differences was ascertained by a two-tailed *t* test.

Results

Initial characterization of GABAergic and putative pyramidal neurons in hippocampal cultures

To examine the distribution of Ca-A/K channels on hippocampal neurons, we produced dissociated hippocampal pure neuronal cultures, plated at low density (so that dendritic trees of many neurons could be visualized unimpeded by neighboring neurons; see Materials and Methods), and examined them after 14–21 d *in vitro*. The presence of Ca-A/K channels was determined by a histochemical labeling technique based on kainate-stimulated uptake of Co²⁺ ions (Co²⁺ labeling). The basis of this technique is that Co²⁺ can permeate Ca-A/K channels but cannot pass through NMDA channels or VSCCs, which represent the other primary routes of agonist-triggered Ca²⁺ entry (Pruss et al., 1991; Yin et al., 1994) (see Materials and Methods). Co²⁺ labeling revealed that Ca-A/K channels were strongly expressed on only a minority (mean ± SEM, 9.0 ± 1.3%; >1500 neurons from six dishes) of neurons in the cultures (Co²⁺(+) neurons).

GABAergic neurons, which are known to possess numerous Ca-A/K channels, were identified by immunolabeling for the enzyme GAD and also constituted a minority (9.0 ± 0.7%; >1500 neurons from six dishes) of the total neuronal population in our cultures. For double labeling, after Co²⁺ loading, cultures were stained for GAD, and microscope fields were photographed before and after Co²⁺ stain development. Most of the Co²⁺(+) neurons (84 ± 1.6%) were also GAD(+), indicating that GABAergic neurons constitute the majority of neurons that possess substantial numbers of Ca-A/K channels in our cultures (Fig. 1A). The Co²⁺(+)/GAD(+) neurons displayed distinctive morphological characteristics. Most (~80%) had large somata (generally 20–25 μm) and smooth-appearing dendrites that branched relatively little. A minority (~5–10%) of these neurons possessed smaller (~15 μm), bipolar-shaped somata but with similar dendritic features. Virtually all of the GAD(+) neurons displayed strong homogeneous Co²⁺ labeling throughout their somata and dendrites.

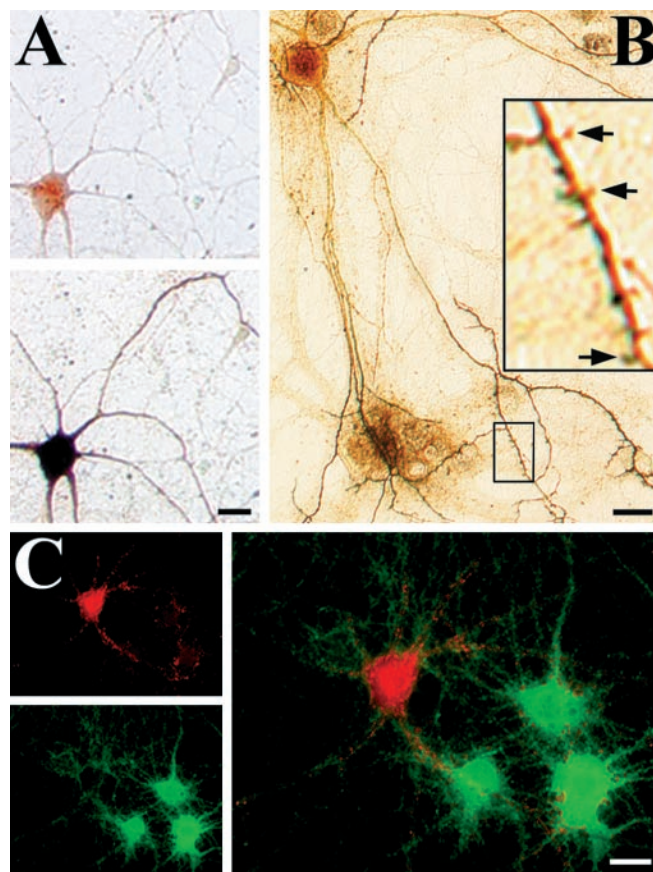GAD(−) neurons in the cultures displayed a number of char-

Figure 1. Kainate-stimulated Co²⁺ uptake labeling and immunohistochemical characterization of cultured hippocampal neurons. *A, B*, Co²⁺ labeling of GABAergic neurons and putative HPNs. Hippocampal cultures were immunolabeled for GAD and subjected to kainate-stimulated Co²⁺ labeling. After photographing the GAD stain, the Co²⁺ stain was developed, and the cells were rephotographed. A representative GAD(+) neuron (*A*, top) with characteristic large soma and smooth, sparsely branching dendrites, is strongly and uniformly Co²⁺(+) (bottom). Although most GAD(−) neurons were also Co²⁺(−), a subset did show Co²⁺ labeling (*B*), which when present was often most evident in the distal dendrites and often extended into apparent dendritic spines (inset, arrows). *C*. CaMKIIα labeling of GABAergic neurons and putative HPNs. A culture was double-immunolabeled for GAD (red) and CaMKIIα (green). Note that CaMKIIα is strongly present in GAD(−) putative HPNs but is mostly absent from the GAD(+) neuron (see overlay, right). Scale bars, 10 μm.

acteristics that distinguished them from GABAergic neurons. First, only a small number of them were Co²⁺(+). However, when Co²⁺ labeling was present, in contrast to the GABAergic neurons, it was usually most evident in the distal dendrites, with staining often visible in apparent dendritic spines (Fig. 1B), whereas somatic labeling was relatively weak. This pattern of Co²⁺ staining was previously observed in HPNs in dissociated murine hippocampal cultures and in acute brain slices (Yin et al., 1999) and suggests the presence of dendritic Ca-A/K channels in a subset of putative HPNs in our cultures. These putative HPNs were morphologically distinct from the GABAergic neurons. Most putative HPNs (>90%) possessed medium-sized (10–20 μm) somata of variable but generally round shape. In addition, they usually had a distinctively flat appearance in contrast to the more convex somata of the GAD(+) neurons, and their dendrites generally possessed numerous fine, distal branches. These morphological criteria for putative HPNs are in agreement with HPNs described in a previous study of cultured hippocampal neurons (Craig et al., 1993). Further establishing the likelihood that these neurons are HPNs, GAD(−) neurons possessing

these morphological features almost always (87%; $n = 83$) expressed high levels of CaMKIIα, an enzyme marker that is reported to be primarily restricted to principal neurons in the hippocampus (Liu and Jones, 1997; Sik et al., 1998), whereas almost all GAD(+) neurons (95%; $n = 60$) lacked CaMKIIα labeling (Fig. 1C).

Detection of Ca-A/K channels using fluorescent Ca^{2+} imaging

We next set out to assess the expression and subcellular distribution of Ca-A/K channels on live neurons using high-resolution fluorescence Ca^{2+} imaging. The cultures were loaded with the low-affinity fluorescent Ca^{2+} probe fluo-4ff AM (K_d, 9.7 μM), and a micropipette containing AMPA (25 μM) along with the NMDA blocker MK-801 and the VSCC antagonist Gd^{3+} (each at 10 μM) was placed adjacent to a visually selected neuron, which was subjected to a brief (1 sec) AMPA pulse. Images were acquired every 0.3 sec for 10 sec and at lower frequencies thereafter. A low-affinity dye was chosen to selectively resolve areas of particularly high intracellular $[Ca^{2+}]$ ($[Ca^{2+}]_i$) rises and thus to provide better localization of Ca^{2+} entry sites than would be possible with high-affinity probes.

In a subpopulation of >270 neurons imaged, AMPA stimulation induced rises in fluo-4ff fluorescence (ΔF) that were usually first evident as discrete dendritic regions of $[Ca^{2+}]_i$ rises flanked by areas of lower $[Ca^{2+}]_i$ that we termed "Ca^{2+} hot spots" (localized ΔF, >1.1 occurring within 0.3 sec; see Materials and Methods). Dendritic $[Ca^{2+}]_i$ rises were typically followed by increases in the soma 1–2 sec later. $[Ca^{2+}]_i$ levels peaked between 10 and 20 sec and usually recovered to near basal levels within ~2–5 min (Fig. 2A, i–iii). The reasons for the prolonged $[Ca^{2+}]_i$ rise after a 1 sec AMPA exposure are incompletely understood but likely reflect some delay in the complete agonist clearance from the field as well as the effects of competition between endogenous Ca^{2+} buffering sites, such as the endoplasmic reticulum (ER), mitochondria, and Ca^{2+}-binding peptides, and the fluorescent probe (Neher, 1995).

In most neurons (82%; 27 of 33) in which basal somatic fluo-4ff fluorescence increased by ΔF of >2.0 within 15 sec of the AMPA exposure, the presence of Ca-A/K channels could be confirmed by somatic as well as dendritic Co^{2+} staining (Fig. 2A, iv); neurons meeting these imaging response criteria were considered Ca-A/K(+) (see Materials and Methods). To further test the specificity of the AMPA-triggered $[Ca^{2+}]_i$ rises for the presence of Ca-A/K channels, in some experiments, AMPA was reapplied in the presence of the Ca-A/K channel antagonist NAS (300 μM; Koike et al., 1997) or the AMPAR antagonist GYKI 52466 (100 μM; Paternain et al., 1995). In seven of eight (NAS) or all 16 experiments (GYKI), the antagonists reversibly abolished the AMPA-induced $[Ca^{2+}]_i$ rise (Fig. 2B). Finally, the AMPA-induced $[Ca^{2+}]_i$ rises were not observed in 0 Ca^{2+} buffer, nor were they reproduced by application of thapsigargin alone, indicating that they were not caused by release of intracellular Ca^{2+} stores (data not shown).

To examine whether the Ca^{2+} hot spots occurred at sites of synapses, we labeled imaged neurons with the synaptic marker synaptophysin. Suggesting that this is indeed the case, the presence of this marker was strongly correlated with the location of dendritic hot spots in five of five neurons examined (Fig. 3A). The Ca^{2+} hot spots were also observed to correlate with spots of surface GluR1 immunoreactivity (Fig. 3B). Taken together, these data strongly suggest that in this system, measured $[Ca^{2+}]_i$ rises
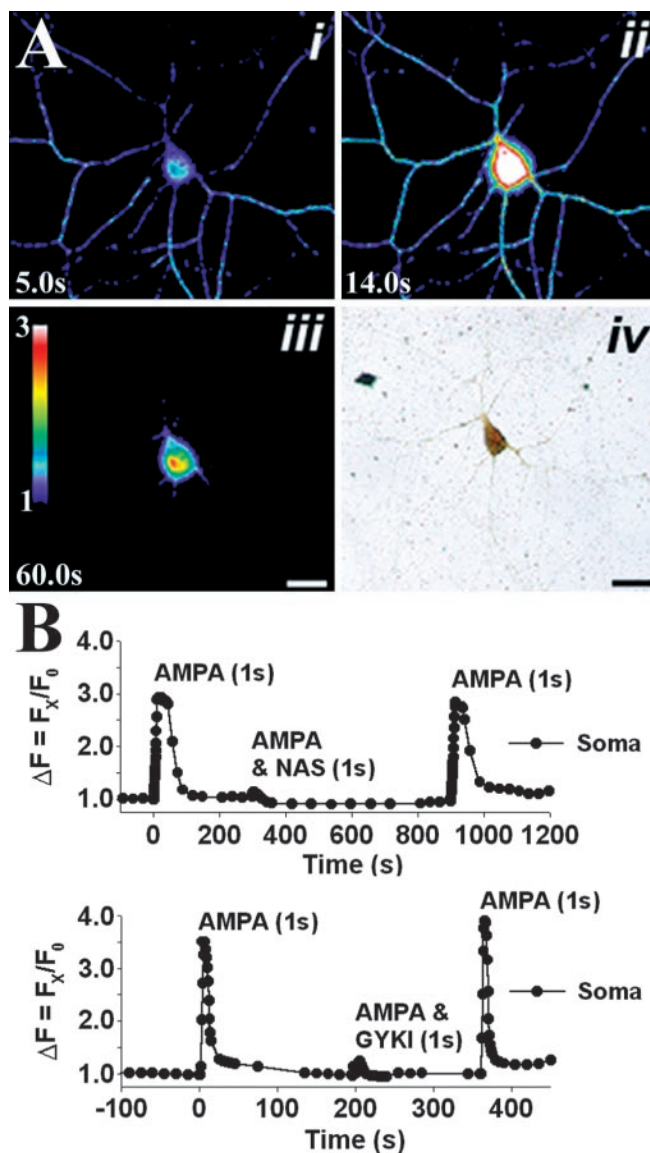

Figure 2. Detection of Ca-A/K channels using fluorescence Ca^{2+} imaging. A, Pseudocolor images. Neurons were loaded with the low-affinity fluorescent Ca^{2+} probe fluo-4ff and exposed to a brief pulse (1 sec) of AMPA (25 μM) in the presence of MK-801 and Gd^{3+} (both at 10 μM). Images represent ΔF in a responding neuron at the times indicated after onset of the exposure (i–iii) and bright-field appearance of the neuron after Co^{2+} labeling (iv). Most neurons (82%; $n = 33$) that (like this one) displayed substantial AMPA-induced somatic $[Ca^{2+}]_i$ rises (ΔF, >2.0) were Co^{2+}(+). The color calibration bar shows pseudocolor mapping of ΔF (applies to all pseudocolor Ca^{2+} images). Scale bars, 10 μm. B, Reversible block of $[Ca^{2+}]_i$ rises by Ca-A/K channel and AMPAR antagonists: traces of representative single-cell responses. After an initial AMPA pulse, selected responding neurons were exposed to a second AMPA pulse in the presence of the Ca-A/K channel blocker NAS (300 μM; top), or the selective AMPAR antagonist GYKI 52466 (100 μM; bottom), followed by a third pulse of AMPA alone.

were in large part attributable to Ca^{2+} entry specifically through synaptically localized Ca-A/K channels.

Distinct patterns of $[Ca^{2+}]_i$ rises in GABAergic neurons versus putative HPNs

In >90% of cells with the above-described morphological characteristics of GABAergic neurons (large, convex soma and sparsely branched dendrites), AMPA stimulation induced strong dendrosomatic $[Ca^{2+}]_i$ rises, with peak ΔF occurring after 15–20 sec and a high percentage exceeding ΔF of 2.0 in both the soma
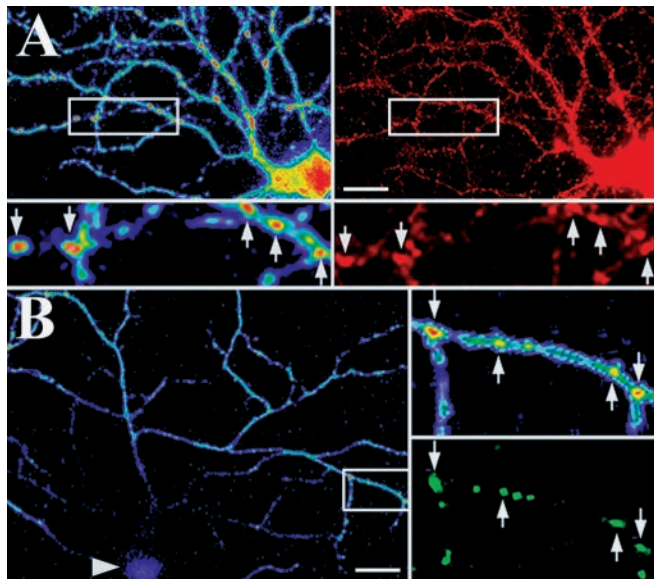
Figure 3. Colocalization of Ca²⁺ hot spots with synaptophysin and GluR1 puncta. *A*, Colocalization with synaptophysin. After AMPA exposure and generation of pseudocolor images of ΔF (left), neurons were stained for the synaptic marker synaptophysin (right); bottom panels show blowups of areas in rectangles. Note the strong overlap between Ca²⁺ hot spots and synaptophysin puncta (arrows). *B*, Colocalization with GluR1. Similarly, after imaging (pseudocolor image on left), this culture was stained for cell surface GluR1; right panels show blowups of the area indicated, showing a ΔF pseudocolor image (top) and GluR1 labeling (bottom). Note the overlap between Ca²⁺ hot spots and GluR1 puncta (arrows). Scale bars, 10 μm.

Figure 4. Distinct pattern of AMPA-induced [Ca²⁺]$_i$ rises in GABAergic neurons and putative HPNs. Cells were puffed with AMPA for 1 sec (*i, ii*, pseudocolor images of ΔF at the times indicated after onset of the exposure) followed by Co²⁺ loading, GAD immunocytochemistry (*iii*, inset), and development of the Co²⁺ stain (*iii*) as described. Note that the GAD(+) neuron (*A*) showed strong dendrosomatic [Ca²⁺]$_i$ rises and correspondingly strong Co²⁺ labeling, whereas the GAD(−) putative HPN (*B*) displayed prominent localized dendritic responses that corresponded to areas of dendritic Co²⁺ labeling (*B, ii, iii*, arrows), before onset of substantial somatic [Ca²⁺]$_i$ rises.

and dendrites (Fig. 4*A, i, ii*). These neurons typically displayed strong Co²⁺ staining, and most (82%; 36 of 44) were retrospectively confirmed by GAD staining to be GABAergic (Fig. 4*A, iii*).

In neurons identified by morphological criteria as probable HPNs, AMPA stimulation triggered a range of responses. A majority showed little or no [Ca²⁺]$_i$ rises in either dendrites or somata [Ca-A/K(−) HPNs]. However, a subset (~22%) displayed numerous (>10 and often 40–50) discrete Ca²⁺ hot spots that were most prominent in the distal dendrites (appearing within 0.3 sec and reaching peak levels at 5–6 sec), generally with smaller and more delayed somatic [Ca²⁺]$_i$ rises (Fig. 4*B, i, ii*). In these neurons, as in the GABAergic neurons, peak ΔF exceeded 2.0 in both the Ca²⁺ hot spots and the soma. Co²⁺ labeling in these neurons was always lighter than that in GAD(+) neurons and sometimes revealed a distinct discontinuous pattern of dendritic staining corresponding to the Ca²⁺ hot spots, and most of these neurons (96%; 23 of 24) were retrospectively confirmed to be GAD(−) [Ca-A/K(+) HPNs; Fig. 4*B, iii*]. These Ca-A/K(+) HPNs were well represented across the age range (14–21 d *in vitro*) of neurons studied.

Comparing parameters of AMPA-triggered [Ca²⁺]$_i$ rises between GABAergic neurons and Ca-A/K(+) HPNs revealed certain distinct differences: (1) [Ca²⁺]$_i$ rises in the GABAergic neurons were slower, with somatic ΔF of 2.0 and peak levels achieved at 11.0 ± 0.9 and 19.1 ± 1.0 sec, respectively ($n = 27$), whereas the HPNs reached these levels at 6.0 ± 1.4 and 11.8 ± 1.7 sec ($n = 23$) respectively; and (2) examining the same set of cells, in GABAergic neurons, the peak dendritic and somatic levels were closely matched (ΔF, 3.2 ± 0.2 and 3.1 ± 0.2 in dendrites and somata, respectively). In contrast, in Ca-A/K(+) HPNs, peak dendritic [Ca²⁺]$_i$ rises were far higher than those in the somata (ΔF, 3.4 ± 0.2 in dendrites vs 2.4 ± 0.2 in the soma).
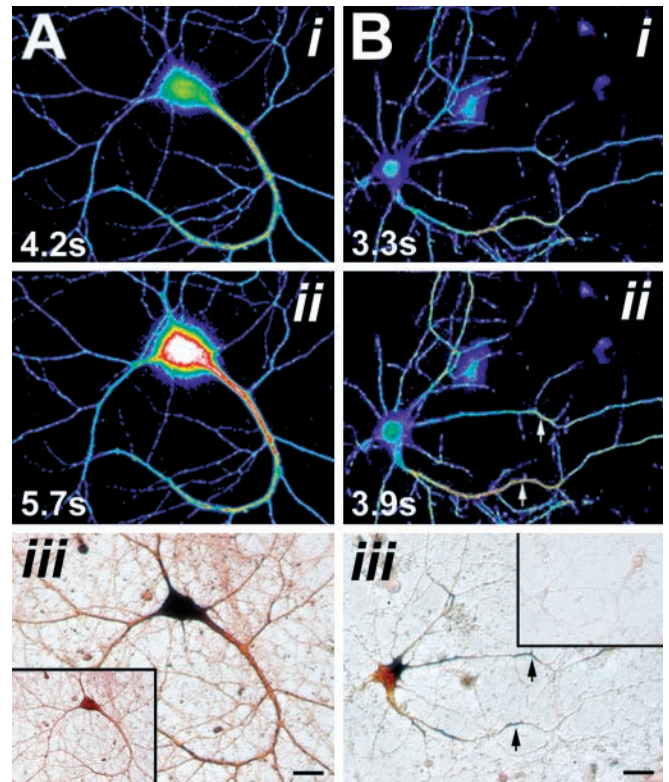
AMPAR subunit surface expression patterns

AMPAR subunit surface expression patterns were determined using a live-cell immunostaining protocol with antibodies directed toward the extracellular N-terminal domains of the GluR1 and GluR2 AMPAR subunits. After AMPAR labeling, neurons were processed for GAD staining. Because of the possibility that relative GluR1 versus GluR2 staining intensities could vary from experiment to experiment as a result of subtle differences in primary and secondary antibody exposures, key comparisons were made between cells in the same dish before trying to generalize across stainings (see Materials and Methods).

GABAergic neurons, identified by GAD staining and morphology, typically possessed punctate dendritic and diffuse somatic GluR1 staining, whereas GluR2 was limited to diffuse staining in the soma and proximal dendritic shafts and did not colocalize well with GluR1 puncta (Fig. 5*A*). GluR1 puncta were distributed along the dendritic shafts, as previously described (Craig et al., 1993). Consistent with a recent study on a subset of parvalbumin-containing neurons (Moga et al., 2002), a subpopulation of GAD(+) neurons appeared to possess no detectable cell surface GluR2 (data not shown).

In contrast to the GABAergic neurons, putative HPNs typically displayed punctate GluR1 and GluR2 surface staining that colocalized extensively on apparent dendritic spines (Fig. 5*B*). The somata of HPNs displayed diffuse surface labeling for both subunits. In a subset of putative HPNs, although GluR1 labeling was still strong in dendritic spines, GluR2 surface expression was
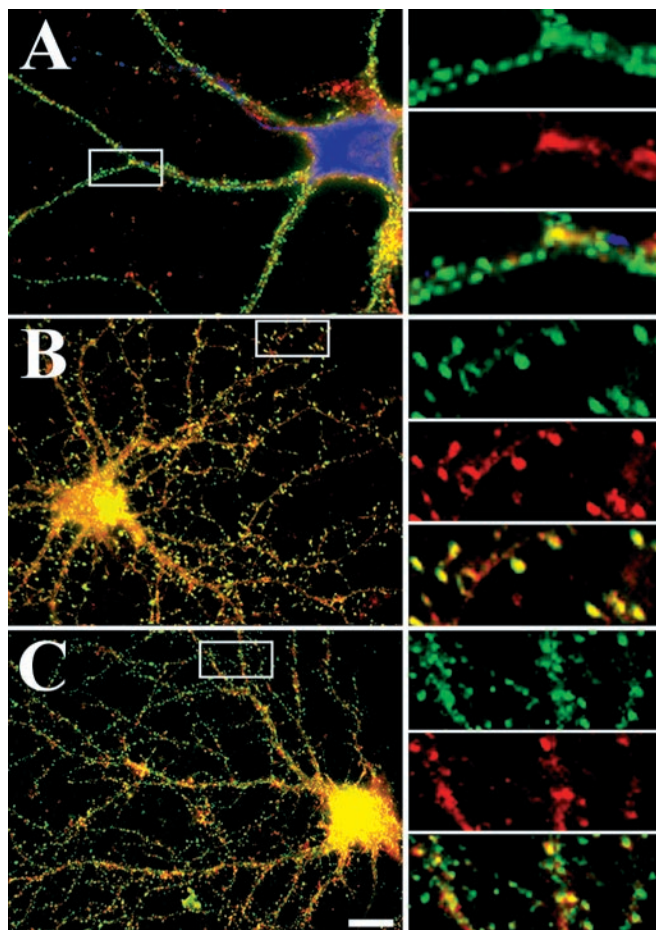
Figure 5. Surface expression patterns of AMPAR subunits in hippocampal neurons. Neurons were triple-labeled for surface GluR1 (green), surface GluR2 (red), and GAD (blue) and examined for differences in the pattern of GluR staining. Right panels show blowup of areas in rectangles, displaying GluR1 (top), GluR2 (middle), and overlap (bottom). *A*, GAD(+) neurons typically displayed strong and abundant dendritic GluR1 puncta along the dendritic shaft, whereas GluR2 labeling was generally limited to the soma and proximal dendritic shafts. *B*, Most putative HPNs possessed abundant dendritic GluR1 and GluR2 puncta that colocalized extensively and was most evident at a distance from the shaft on apparent dendritic spines. *C*, A subset of putative HPNs, however, displayed large numbers of puncta in which GluR1 labeling was predominant. Scale bar, 10 μm.

Figure 6. Correlation between AMPA-induced [Ca²⁺]ᵢ rises and AMPAR subunit surface expression in a GABAergic neuron. Top, The pseudocolor image displays peak [Ca²⁺]ᵢ rises after a 1 sec AMPA application. Bottom, After imaging, the cell was triple-labeled for surface GluR1 (green), surface GluR2 (red), and GAD (blue). Note the strong [Ca²⁺]ᵢ rise throughout the cell corresponding to strong punctate dendritic GluR1 labeling, with little GluR2. Also note that the atypical GAD(−) putative HPN in the top left corner, which displays prominent dendritic GluR2 with little GluR1, did not display any detectable [Ca²⁺]ᵢ rise on AMPA application, presumably because of an absence of Ca-A/K channels. Scale bar, 10 μm.

relatively low (Fig. 5C). A wide range of staining patterns was observed in all cultures examined.

Correlation between Ca-A/K channel and AMPAR subunit distribution on the same neuron

In some experiments, Ca²⁺ imaging assessment of Ca-A/K channels was followed by cell surface AMPAR subunit immunostaining. In GABAergic neurons, we found the [Ca²⁺]ᵢ responses and patterns of cell surface labeling described above to be invariably observed in the same neurons, with strong dendrosomatic [Ca²⁺]ᵢ rises and GluR1-predominant puncta along the dendritic shafts (Fig. 6).

In Ca-A/K(−) HPNs, surface AMPAR subunit labeling revealed that GluR1 and GluR2 colocalized (Fig. 7A). [There were also rare Ca-A/K(−) HPNs that showed strong GluR2 but little GluR1 labeling (see Fig. 6)]. In the Ca-A/K(+) HPNs, however, immunolabeling revealed much stronger and more abundant GluR1 staining compared with GluR2 (Fig. 7B).

Although the spatial resolution of the techniques would not permit a spot-to-spot correlation between the AMPAR composi-
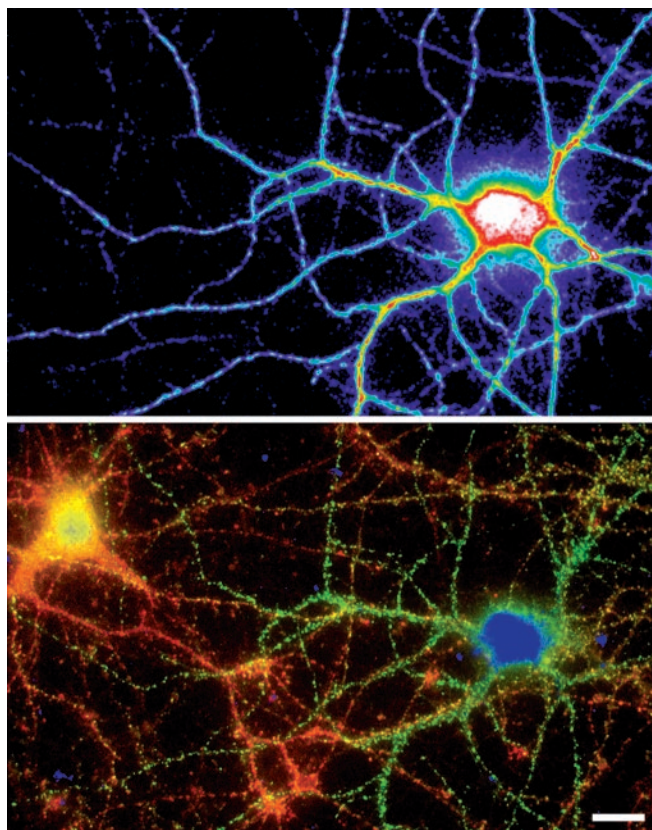
tion of individual puncta and localized [Ca²⁺]ᵢ rises, two approaches were used to further characterize the relationship between cell surface GluR1 and GluR2 and the presence of Ca-A/K channels in HPNs (see Materials and Methods). First, we compared the average overall intensity of GluR1 and GluR2 fluorescence in the dendrites for each neuron subjected to both AMPAR immunocytochemistry and imaging. We found that Ca-A/K(+) HPNs had significantly greater GluR1/GluR2 fluorescence ratios (2.0 ± 0.4; $n = 7$) than Ca-A/K(−) HPNs (1.2 ± 0.1; $n = 11$; Fig. 8A). Although these measures do not reflect actual ratios of GluR1 and GluR2 protein levels, they nonetheless provide information as to the relative differences in their expression levels between Ca-A/K(+) and Ca-A/K(−) HPNs. Second, we counted numbers of puncta (∼250–300 puncta per neuron) in the dendrites of each of these neurons in which GluR1 labeling was clearly stronger than GluR2 (GluR1 > GluR2) and those in which GluR2 labeling was greater than or equal to GluR1 (GluR2 ≥ GluR1). We found Ca-A/K(+) HPNs to possess a significantly higher percentage of GluR1 > GluR2 puncta (61 ± 4%) than Ca-A/K(−) HPNs (23 ± 4%; Fig. 8B). Thus, although HPNs generally possess high levels of both subunits, the presence of Ca-A/K channels appears to be a function of the amount of cell surface GluR1 relative to that of GluR2.
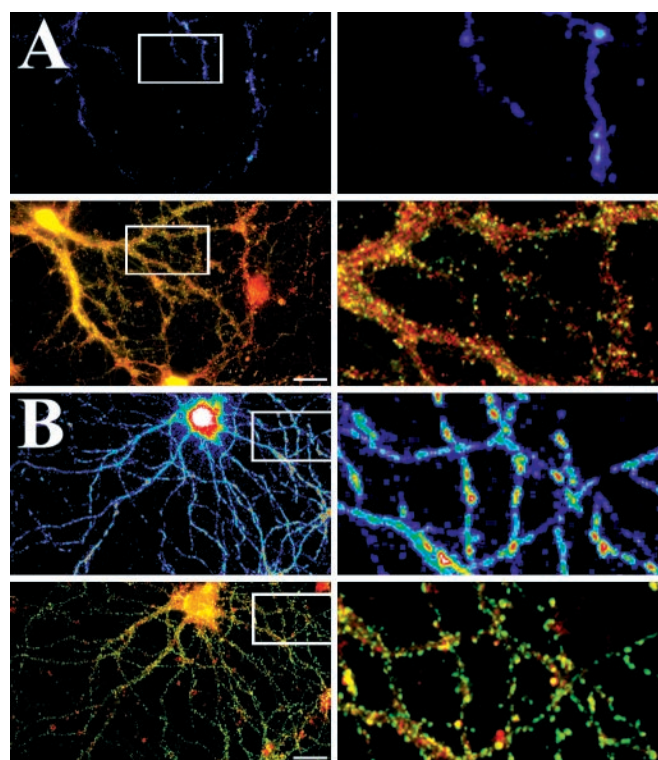
Figure 7. Correlation between AMPA-induced $[Ca^{2+}]_i$ rises and AMPAR subunit surface expression in putative HPNs. Hippocampal neurons were imaged after a 1 sec AMPA exposure (top panels), followed by triple immunofluorescence labeling for GluR1, GluR2, and GAD (bottom panels). In a Ca-A/K(−) HPN (*A*), GluR1 (green) and GluR2 (red) puncta colocalize extensively. In contrast, in a Ca-A/K(+) HPN (*B*), GluR1 is strongly present in many puncta along with little or no GluR2. Scale bars, 10 μm.

Figure 8. Ca-A/K(+) HPNs have greater dendritic GluR1 relative to GluR2 than Ca-A/K(−) HPNs: quantitative assessments. *A*, Averaged dendritic GluR1 and GluR2 fluorescence. Neurons were imaged followed by triple immunolabeling, and average raw fluorescence intensity of GluR1 and GluR2 was measured in the dendrites of each neuron. Bars show mean GluR1/GluR2 fluorescence ratios in Ca-A/K(+) and Ca-A/K(−) HPNs. *Fluorescence ratio greater than that in Ca-A/K(−) neurons; $p < 0.05$ ($n = 11$ Ca-A/K(−), 7 Ca-A/K(+) HPNs). *B*. Counting and characterization of puncta. After imaging, GluR1 and GluR2 labeling patterns in the same set of neurons were also assessed by counting all evident discrete puncta in the dendrite of each neuron and categorizing each one as GluR1-predominant (GluR1 > GluR2) or as showing labeling for GluR2 at least as strong as for GluR1 (GluR2 ≥ GluR1). *Percent GluR1 > GluR2" puncta significantly greater than in Ca-A/K(−) HPNs; $p < 0.0001$.

Discussion
Principal findings
This study used a simplified culture system to examine the presence of Ca-A/K channels and of the AMPAR subunits GluR1 and GluR2 in hippocampal neurons. Assessing the presence of functional Ca-A/K channels as acute $[Ca^{2+}]_i$ rises on AMPA exposure in the presence of NMDA channel and VSCC blockade, we find that these channels only appear to be present on a subpopulation of hippocampal neurons. We further find distinct differences in the characteristics of $[Ca^{2+}]_i$ rises between GABAergic neurons and putative HPNs. Whereas GABAergic neurons virtually always showed strong but slowly rising dendrosomatic responses, HPNs had very heterogeneous responses, with only ~20% having apparent Ca-A/K channels but which, when present, gave relatively fast $[Ca^{2+}]_i$ rises that were most evident on dendrites. Furthermore, the present study is the first to examine the relationship between the distributions of surface AMPAR subunits with that of functional Ca-A/K channels on the same neuron and demonstrates that HPNs possessing numerous Ca-A/K channels have far greater levels of cell surface GluR1 relative to GluR2 than those apparently lacking substantial numbers of these channels.

Finally, given the presence of cell surface GluR2 throughout the somata and dendrites of virtually all HPNs, the present findings provide new direct confirmation of the idea that Ca²⁺-permeable and -impermeable AMPA channels often coexist on the same cell, and expression of considerable cell surface GluR2 peptide does not preclude the presence of Ca-A/K channels.
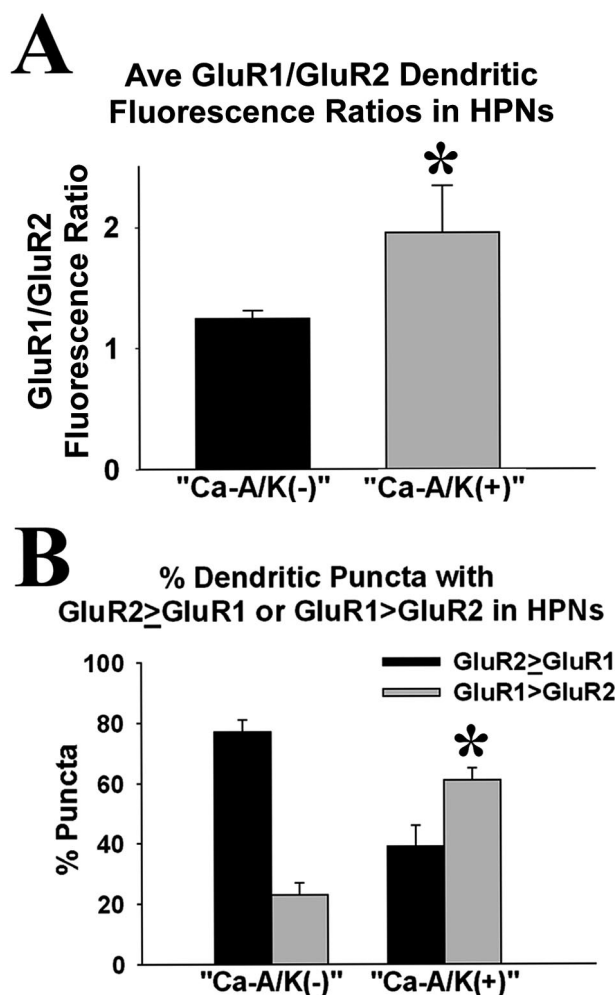
Presence of Ca-A/K channels on HPNs
Although many forebrain GABAergic neurons are well documented to possess large numbers of Ca-A/K channels, understanding of their expression patterns on HPNs is far more limited. This may reflect in part both the nature of the techniques used to assess their presence and the complexity of channel expression patterns on these neurons. Indeed, with one exception (Lerma et al., 1994), electrophysiological studies have provided little evidence for the presence of Ca-A/K channels on HPNs, and the high levels of GluR2 mRNA and protein invariably found in HPNs have been used to argue against their substantial presence. Thus, it seems clear that if Ca-A/K channels are present on HPNs, they likely constitute a small minority of total AMPA channels present.

However, it has become increasingly apparent that Ca²⁺-permeable and -impermeable AMPA channels can often coexist

on the same neuron. Underlying this changing view are numerous studies indicating that GluR1/GluR2 mRNA expression ratios vary widely, and these ratios generally predict relative Ca^{2+} permeability of AMPA channels, as assessed by electrophysiological assessment of the degree of inward rectification (Iino et al., 1994; Geiger et al., 1995; Goldstein et al., 1995; Zhang et al., 1995; Isa et al., 1996; Washburn et al., 1997).

Positive evidence for the presence of Ca-A/K channels on HPNs under basal conditions has primarily been based on observations of kainate-stimulated Co^{2+} uptake labeling (Pruss et al., 1991; Toomim and Millington, 1998; Yin et al., 1999). Indeed, the finding that the Co^{2+} accumulation frequently appeared to occur in dendrites but not in apparent axons of cultured neurons (Yin et al., 1999) and observations that different populations of neurons show distinctly differing patterns of labeling, with some showing strong dendrosomatic staining and others showing discrete areas of labeling in the dendrites but little in the somata, support the idea that the stain provides some information as to the subcellular localization of Ca-A/K channels. Furthermore, this technique, like the imaging approaches used in this study, may be able to detect low levels of Ca-A/K channels with greater sensitivity than electrophysiology. Specifically, whereas whole-cell recording is biased to favor currents closer to the soma and provides information as to the relative contribution of Ca-A/K channels to total AMPA current, Co^{2+} labeling or fluorescence imaging provides information about the presence of Ca-A/K channels over the entire dendritic tree, irrespective of the relative number of Ca^{2+}-impermeable channels. Thus, it is our contention that HPNs often possess a limited number of Ca-A/K channels, but when present, they are preferentially found in dendrites, where they are functionally important for synaptic signaling but are hard to detect electrophysiologically.

Functional significance

There is presently little known about the specific physiological roles of Ca-A/K channels. Several studies have suggested that Ca^{2+} entry through these channels may mediate forms of synaptic plasticity in GABAergic and possibly some other types of neurons (Gu et al., 1996; Mahanty and Sah, 1998; Toth and McBain, 1998; Liu and Cull-Candy, 2000, 2002; Ross and Soltesz, 2001), although evidence for such roles of Ca-A/K channels specifically present on HPNs is presently lacking.

One of the key observations of the present study is that the numbers and distribution of Ca-A/K channels among HPNs appear to be extremely variable, with some virtually lacking them and others having considerable numbers in discrete regions of their dendrites. Given that the present observations show the distribution of Ca-A/K channels on HPNs at a fixed point in time, they are compatible with the idea that the numbers of these channels are in dynamic flux, possibly changing in response to synaptic activity. Indeed, neurons do possess considerable machinery to regulate the presence of synaptic AMPA channels, which can traffic into and out of synapses in response to physiological stimulation (Malinow and Malenka, 2002; Song and Huganir, 2002). Furthermore, much of this machinery appears to have specificity for GluR2 subunits; an ER mechanism was even found that appears to detect the region of GluR2 that controls Ca^{2+} permeability (Greger et al., 2002), suggesting that the insertion of the GluR2 subunit and thus production of Ca-A/K channels are highly regulated. However, regulation of Ca-A/K channels in response to physiological stimuli has been studied little and to date has been observed in only one study, in cerebellar neurons (Liu and Cull-Candy, 2000).

If Ca-A/K channels in HPNs subserve specific physiological functions, certain features of these channels may differentiate them from NMDA channels in terms of their potential roles in plasticity. First, they are not subject to a voltage-dependent block by Mg^{2+} ions and are opened on glutamate activation irrespective of the postsynaptic membrane potential. In addition, as discussed above, they are highly permeable to Zn^{2+} ions, which are synaptically released at many excitatory pathways (Frederickson, 1989), yet block NMDA channels (Peters et al., 1987; Westbrook and Mayer, 1987). Thus, Ca-A/K channels may serve as critical routes for trans-synaptic Zn^{2+} signaling, a mechanism that has been suggested to contribute to long-term potentiation (Weiss et al., 1989; Lu et al., 2000; Li et al., 2001).

Furthermore, presently observed differences in the distribution of and [Ca^{2+}]$_i$ responses to Ca-A/K channel activation between HPNs and GABAergic neurons may suggest differing roles of divalent cation (Ca^{2+} or Zn^{2+}) signaling through Ca-A/K channels in these two cell types. Specifically, findings of relatively slow and widespread [Ca^{2+}]$_i$ rises in GABAergic neurons may be compatible with their strong expression of various Ca^{2+}-binding proteins (Kawaguchi and Hama, 1988; Freund and Buzsaki, 1996) and may possibly reflect an ability of the cell to integrate Ca^{2+} rises over time. This may be well suited for signaling at the level of cell output by modifying excitability, as has indeed been suggested in the case of Ca-A/K channel activation in GABAergic neurons (Ross and Soltesz, 2001). In contrast, when they occur in putative HPNs, [Ca^{2+}]$_i$ rises were faster and more prominent in the dendrites, perhaps compatible with more local signaling at the input side of the cell (Sabatini et al., 2001), as in the case of postsynaptic modification observed in HPNs in response to plasticity-inducing stimuli (Malinow and Malenka, 2002; Song and Huganir, 2002). In addition to their high Ca^{2+} permeability, Ca-A/K channels are characterized by high single-channel conductance (Angulo et al., 1997; Swanson et al., 1997). Thus, the presence of these channels in distal HPN dendrites could conceivably play a role in recently described distance scaling of excitatory inputs (Smith et al., 2003).

Regardless of their physiological roles, there is considerable evidence that Ca-A/K channels play a role in the degeneration of HPNs occurring after ischemia or epilepsy. Indeed, a role for these channels may be suggested by the surprisingly good protection afforded by AMPA/kainate antagonists in models of ischemia (Pulsinelli et al., 1993; Sheardown et al., 1993). The presence of Ca-A/K channels in HPN dendrites could serve as a route for toxic Zn^{2+} accumulation in these conditions (Frederickson et al., 1989; Tonder et al., 1990; Koh et al., 1996; Weiss and Sensi, 2000). Indeed, we have found that the Ca-A/K channel blocker NAS decreased both Zn^{2+} accumulation and HPN cell death in a slice model of ischemia (Yin et al., 2002). Thus, in light of the high toxic potency of Zn^{2+} (Weiss and Sensi, 2000), it is possible that Zn^{2+} released under these conditions could block NMDA channels but permeate Ca-A/K channels, permitting a relatively small number of these channels to induce disproportionate degrees of injury. Furthermore, regardless of their levels under basal conditions, evidence for decreases in GluR2 and consequent increases in numbers of Ca-A/K channels after episodes of transient ischemia or prolonged seizures suggests that these channels may well contribute to the delayed neurodegeneration occurring in these conditions (Tanaka et al., 2000).

Conclusions

These studies provide new insights into the presence and distribution of Ca-A/K channels on distinct populations of central

neurons and their relationship to patterns of cell surface AMPAR subunits. The studies lend support to the idea that HPNs show tremendous heterogeneity in terms of their Ca-A/K channel expression and that, when present, they are disproportionately located in dendrites. These observations, taken together with previous clues suggesting that numbers of Ca-A/K channels are likely to be amenable to regulation under physiological or pathophysiological conditions, set the stage for future studies to more fully understand their roles in disease and physiological signaling.

References

Angulo MC, Lambolez B, Audinat E, Hestrin S, Rossier J (1997) Subunit composition, kinetic, and permeation properties of AMPA receptors in single neocortical nonpyramidal cells. J Neurosci 17:6685–6696.

Brewer GJ, Torricelli JR, Evege EK, Price PJ (1993) Optimized survival of hippocampal neurons in B27-supplemented Neurobasal, a new serum-free medium combination. J Neurosci Res 35:567–576.

Bochet P, Audinat E, Lambolez B, Crepel F, Rossier J, Iino M, Tsuzuki K, Ozawa S (1994) Subunit composition at the single-cell level explains functional properties of a glutamate-gated channel. Neuron 12:383–388.

Craig AM, Blackstone CD, Huganir RL, Banker G (1993) The distribution of glutamate receptors in cultured hippocampal neurons: postsynaptic clustering of AMPA-selective subunits. Neuron 10:1055–1068.

Frederickson CJ (1989) Neurobiology of zinc and zinc-containing neurons. Int Rev Neurobiol 31:145–238.

Frederickson CJ, Hernandez MD, McGinty JF (1989) Translocation of zinc may contribute to seizure-induced death of neurons. Brain Res 480:317–321.

Freund TF, Buzsaki G (1996) Interneurons of the hippocampus. Hippocampus 6:347–470.

Garaschuk O, Shneggenburger R, Schirra C, Tempia F, Konnerth A (1996) Fractional Ca²⁺ currents through somatic and dendritic glutamate receptor channels of rat hippocampal CA1 pyramidal neurones. J Physiol (Lond) 491:757–772.

Geiger JRP, Melcher T, Koh DS, Sakmann B, Seeburg PH, Jonas P, Monyer H (1995) Relative abundance of subunit mRNAs determines gating and Ca²⁺ permeability of AMPA receptors in principal neurons and interneurons in rat CNS. Neuron 15:193-204.

Goldstein PA, Lee CJ, MacDermott AB (1995) Variable distributions of Ca(2+)-permeable and Ca(2+)-impermeable AMPA receptors on embryonic rat dorsal horn neurons. J Neurophysiol 73:2522–2534.

Greger IH, Khatri L, Ziff EB (2002) RNA editing at arg607 controls AMPA receptor exit from the endoplasmic reticulum. Neuron 34:759–772.

Gu JG, Albuquerque C, Lee CJ, MacDermott AB (1996) Synaptic strengthening through activation of Ca²⁺-permeable AMPA receptors. Nature 381:793–796.

Hollmann M, Hartley M, Heinemann S (1991) Ca²⁺ permeability of KA-AMPA-gated glutamate receptor channels depends on subunit composition. Science 252:851–853.

Iino M, Ozawa S, Tsuzuki K (1990) Permeation of calcium through excitatory amino acid receptor channels in cultured rat hippocampal neurones. J Physiol (Lond) 424:151–165.

Iino M, Mochizuki S, Ozawa S (1994) Relationship between calcium permeability and rectification properties of AMPA receptors in cultured rat hippocampal neurons. Neurosci Lett 173:14–16.

Isa T, Itazawa S, Iino M, Tsuzuki K, Ozawa S (1996) Distribution of neurones expressing inwardly rectifying and Ca(2+)-permeable AMPA receptors in rat hippocampal slices. J Physiol (Lond) 491:719–733.

Jia Y, Jeng JM, Sensi SL, Weiss JH (2002) Zn²⁺ currents are mediated by calcium-permeable AMPA/kainate channels in cultured murine hippocampal neurones. J Physiol (Lond) 543:35–48.

Jonas P, Racca C, Sakmann B, Seeburg PH, Monyer H (1994) Differences in Ca²⁺ permeability of AMPA-type glutamate receptor channels in neocortical neurons caused by differential GluR-B subunit expression. Neuron 12:1281–1289.

Kawaguchi Y, Hama K (1988) Physiological heterogeneity of nonpyramidal cells in rat hippocampal CA1 region. Exp Brain Res 72:494–502.

Koh JY, Suh SW, Gwag BJ, He YY, Hsu CY, Choi DW (1996) The role of zinc in selective neuronal death after transient global cerebral ischemia. Science 272:1013–1016.

Koike M, Iino M, Ozawa S (1997) Blocking effect of 1-naphthyl acetyl

spermine on Ca(2+)-permeable AMPA receptors in cultured rat hippocampal neurons. Neurosci Res 29:27–36.

Lerma J, Morales M, Ibarz JM, Somohano F (1994) Rectification properties and Ca2+ permeability of glutamate receptor channels in hippocampal cells. Eur J Neurosci 6:1080–1088.

Li Y, Hough CJ, Frederickson CJ, Sarvey JM (2001) Induction of mossy fiber → Ca3 long-term potentiation requires translocation of synaptically released Zn²⁺. J Neurosci 21:8015–8025.

Liu SQ, Cull-Candy SG (2000) Synaptic activity at calcium-permeable AMPA receptors induces a switch in receptor subtype. Nature 405:454–458.

Liu SJ, Cull-Candy SG (2002) Activity-dependent change in AMPA receptor properties in cerebellar stellate cells. J Neurosci 22:3881–3889.

Liu X, Jones EG (1997) Alpha isoform of calcium-calmodulin dependent kinase II (CAM II kinase-) restricted to excitatory synapses in the CA1 region of rat hippocampus. NeuroReport 8:1475–1479.

Lu YM, Taverna FA, Tu R, Ackerley CA, Wang YT, Roder J (2000) Endogenous Zn(2+) is required for the induction of long-term potentiation at rat hippocampal mossy fiber-CA3 synapses. Synapse 38:187–197.

Mahanty NK, Sah P (1998) Calcium-permeable AMPA receptors mediate long-term potentiation in interneurons in the amygdala. Nature 394:683–687.

Malinow R, Malenka RC (2002) AMPA receptor trafficking and synaptic plasticity. Annu Rev Neurosci 25:103–126.

McBain CJ, Dingledine R (1993) Heterogeneity of synaptic glutamate receptors on CA3 stratum radiatum interneurones of rat hippocampus. J Physiol (Lond) 462:373–392.

Moga D, Hof PR, Vissavajihala P, Moran TM, Morrison JH (2002) Parvalbumin-containing interneurons in the rat hippocampus have an AMPA receptor profile suggestive of vulnerability to excitotoxicity. J Chem Neuronanat 23:249–253.

Neher E (1995) The use of fura-2 for estimatintg Ca²⁺ buffers and Ca²⁺ fluxes. Neuropharmacology 34:1423–1442.

Paternain AV, Morales M, Lerma J (1995) Selective antagonism of AMPA receptor unmasks kainate receptor-mediated responses in hippocampal neurons. Neuron 14:185–189.

Pellegrini-Giampietro DE, Zukin RS, Bennett MV, Cho S, Pulsinelli WA (1992) Switch in glutamate receptor subunit gene expression in CA1 subfield of hippocampus following global ischemia in rats. Proc Natl Acad Sci USA 89:10499–10503.

Peters S, Koh J, Choi DW (1987) Zinc selectively blocks the action of N-methyl-D-aspartate on cortical neurons. Science 236:589–593.

Petralia RS, Wang YX, Mayat E, Wenthold RJ (1997) Glutamate receptor subunit 2-selective antibody shows a differential distribution of calcium-impermeable AMPA receptors among populations of neurons. J Comp Neurol 385:456–476.

Pruss RM, Akeson RL, Racke MM, Wilburn JL (1991) Agonist-activated cobalt uptake identifies divalent cation-permeable kainate receptors on neurons and glial cells. Neuron 7:509–518.

Pulsinelli W, Sarokin A, Buchan A (1993) Antagonism of the NMDA and non-NMDA receptors in global versus focal brain ischemia. Prog Brain Res 96:125–135.

Ross ST, Soltesz I (2001) Long-term plasticity in interneurons of the dentate gyrus. Proc Natl Acad Sci USA 98:874–879.

Sabatini BL, Maravall M, Svoboda K (2001) Ca(2+) signaling in dendritic spines. Curr Opin Neurobiol 11:349–356.

Sheardown MJ, Suzdak PD, Nordholm L (1993) AMPA, but not NMDA, receptor antagonism is neuroprotective in gerbil global ischaemia, even when delayed 24 h. Eur J Pharmacol 236:347–353.

Sik A, Hajos N, Gulacsi A, Mody I, Freund TF (1998) The absence of a major Ca2+ signaling pathway in GABAergic neurons of the hippocampus. Proc Natl Acad Sci USA 95:3245–3250.

Smith MA, Ellis-Davies GC, Magee JC (2003) Mechanism of the distance-dependent scaling of Schaffer collateral synapses in rat CA1 pyramidal neurons. J Physiol (Lond) 548:245–258.

Song I, Huganir RL (2002) Regulation of AMPA receptors during synaptic plasticity. Trends Neurosci 25:578–588.

Spruston N, Jonas P, Sakmann B (1995) Dendritic glutamate receptor channels in rat hippocampal CA3 and CA1 pyramidal neurons. J Physiol (Lond) 482:325–352.

Swanson GT, Kamboj SK, Cull-Candy SG (1997) Single-channel properties

of recombinant AMPA receptors depend on RNA editing, splice variation, and subunit composition. J Neurosci 17:58–69.

Tanaka H, Grooms SY, Bennett MV, Zukin RS (2000) The AMPAR subunit GluR2: still front and center-stage. Brain Res 886:190–207.

Tonder N, Johansen FF, Frederickson CJ, Zimmer J, Diemer NH (1990) Possible role of zinc in the selective degeneration of dentate hilar neurons after cerebral ischemia in the adult rat. Neurosci Lett 109:247–252.

Toomim CS, Millington WR (1998) Regional and laminar specificity of kainate-stimulated cobalt uptake in the rat hippocampal formation. J Comp Neurol 402:141–154.

Toth K, McBain CJ (1998) Afferent-specific innervation of two distinct AMPA receptor subtypes on single hippocampal interneurons. Nat Neurosci 1:572–578.

Vandenberghe W, Bindokas VP, Miller RJ, Robberecht W, Brorson JR (2001) Subcellular localization of calcium-permeable AMPA receptors in spinal motoneurons. Eur J Neurosci 14:305–314.

Verdoorn TA, Burnashev N, Monyer H, Seeburg PH, Sakmann B (1991) Structural determinants of ion flow through recombinant glutamate receptor channels. Science 252:1715–1718.

Washburn MS, Numberger M, Zhang S, Dingledine R (1997) Differential dependence on GluR2 expression of three characteristic features of AMPA receptors. J Neurosci 17:9393–9406.

Weiss JH, Sensi SL (2000) Ca2+-Zn2+ permeable AMPA or kainate receptors: possible key factors in selective neurodegeneration. Trends Neurosci 23:365–371.

Weiss JH, Koh JY, Christine CW, Choi DW (1989) Zinc and LTP. Nature 338:212.

Wenthold RJ, Petralia RS, Blahos JII, Niedzielski AS (1996) Evidence for multiple AMPA receptor complexes in hippocampal CA1/CA2 neurons. J Neurosci 16:1982–1989.

Westbrook GL, Mayer ML (1987) Micromolar concentrations of Zn2+ antagonize NMDA and GABA responses of hippocampal neurons. Nature 328:640–643.

Yin H, Turetsky D, Choi DW, Weiss JH (1994) Cortical neurones with Ca2+ permeable AMPA/kainate channels display distinct receptor immunoreactivity and are GABAergic. Neurobiol Dis 1:43–49.

Yin HZ, Sensi SL, Carriedo SG, Weiss JH (1999) Dendritic localization of Ca(2+)-permeable AMPA/kainate channels in hippocampal pyramidal neurons. J Comp Neurol 409:250–260.

Yin HZ, Sensi SL, Ogoshi F, Weiss JH (2002) Blockade of Ca²⁺-permeable AMPA/kainate channels decreases oxygen-glucose deprivation-induced Zn²⁺ accumulation and neuronal loss in hippocampal pyramidal neurons. J Neurosci 22:1273–1279.

Zhang D, Sucher NJ, Lipton SA (1995) Co-expression of AMPA/kainate receptor-operated channels with high and low Ca²⁺ permeability in single rat retinal ganglion cells. Neuroscience 67:177–188.